Sensors & Transducers, Vol. 229, Issue 1, January 2019, pp. 18-23

www.sensorsportal.com

Sensors & Transducers

Published by IFSA Publishing, S. L., 2019
http://www.sensorsportal.com

Nanocomposite H_2O_2 Vapor Sensors Made on the Base of Carbon Nanotubes Covered with SnO_2 Nanoparticles

[1] Zaven ADAMYAN, [1] Artak SAYUNTS, [1] Emma KHACHATURYAN, [1] Valeri ARAKELYAN, [1] Vladimir AROUTIOUNIAN and [2] Bernth JOOST

[1] Yerevan State University, Research Center of Semiconductor Devices and Nanotechnologies, 1 Alex Manoogian, 0025, Yerevan, Armenia

[2] Institute for Pharmaceutical Technology, Fachhochschule Nordwestschweiz, Hochschule für Life Sciences, Gründenstrasse 40, 4132 Muttenz, Switzerland

[1] Tel.: +37460710311, fax: +37460710355

[1] E-mail: zad@ysu.am

Received: 30 November 2018 /Accepted: 31 December 2018 /Published: 31 January 2019

Abstract: In this work, we present the results of studies of the nanocomposite MWCNTs/SnO_2 hydrogen peroxide vapor sensors. The technology of manufacturing these sensors has been developed. As a result of the measurements of the temperature characteristics, the 100°C optimal operating temperature of the studied sensors has been found. The response and recovery curves of the sensors were investigated in the presence of different concentrations of hydrogen peroxide vapor in the atmosphere. Sufficiently high response when low concentrations of the target gas presents in the air is observed. The linear dependence of the sensors response on the concentration of hydrogen peroxide vapor is observed in a double logarithmic scale in a certain concentration range. The minimal registered gas concentration is 1 ppm or less than.

Keywords: H_2O_2 vapor sensor, MWCNTs/SnO_2 Nanocomposite, Carbon nanotubes, Hydrothermal synthesis, Sol-gel.

1. Introduction

Hydrogen peroxide vapors have become a common disinfectant due to their pronounced bactericidal properties [1-2]. Hydrogen peroxide is characterized by a wide range of antibacterial properties, low toxicity. However, hydrogen peroxide vapor belongs to the category of hazardous substances for people who are in a working room with a certain maximum permissible concentration of hydrogen peroxide vapor. Therefore, it is necessary to protect personnel outside the disinfected premises from accidental leakage of H_2O_2 fumes.

With a significant vapor pressure (1.2 kPa at 50°C), hydrogen-peroxide vapor is potentially hazardous and explosive. Recently, the easily made peroxide based explosives most actively used by terrorists groups [3-5]. Therefore both the development of sensors for the detection of H_2O_2 vapor and the determination of their concentration in the environment are very relevant and important.

To date, several techniques have been proposed for the detection of hydrogen peroxide, such as chemiluminescent, spectrophotometric, fluorometric, calorimetric and optical interferometry. All these techniques are complex, expensive and require considerable time consuming. In addition, these methods not always allow to measure low concentrations of H_2O_2 in the range of the threshold limit concentration of 1 ppm. This is seemed possible

and promising in the detection of H_2O_2 vapors using semiconductor metal-oxide gas sensors [6-8] and theirs nanocomposites including carbon nanotubes, different catalysts, metal-phthalocyanines [4, 9-11] and others.

Our previous research works [12-15] have demonstrated that the gas sensors based on the multiwalled carbon nanotubes/tin oxide nanocomposite hybrid materials (MWCNTs/SnO_2) have a good gas sensing performance. The enhancement of the sensing performance is facilitated by the very large specific surface area of these nanocomposites. On the other hand, presence of nanochannels in the form of hollow CNTs for gas diffusion [16] also promotes for improving of the gas sensing characteristics of such nanocomposite. Moreover, it is known that the n-p heterojunctions are formed at the interface between tin oxide nanoparticles and carbon nanotubes since SnO_2 is n-type semiconductor whereas carbon nanotubes form p-type semiconductor [17]. The adsorption of gas molecules changes both the depletion layers at the surface of SnO_2 nanoparticles and at the p-MWCNTs/n-SnO_2 heterojunctions. The existence of this heterojunction also should contribute to an increase in the signal of the sensor.

Surface modification of the CNTs/metal-oxide hybrid gas sensors and sensors based on the nanocomposites components with noble metals, especially with Ru, promotes increasing in sensitivity and improvement of the gas sensors speed performance [18–20] because of these metals or their oxides are the catalysts for chemical reactions taking place on the surface. So, high sensitivity, good selectivity and lower operating temperatures achieve for Ru incorporated SnO_2/MWCNTs nanocomposites based various alcohols and hydrocarbon gas sensors [12-16, 20-21].

All these mentioned above facts and effects promote to sensing and improving the characteristics of the MWCNTs/SnO_2 gas sensors to hydrogen peroxide vapor. In this paper we present some results of these investigations.

2. The Technology of the SnO_2/MWCNTs Nanocomposite Gas Sensors

We have developed two types of samples sensitive to hydrogen peroxide vapors, which are presented below.

2.1. The Ruthenated Nanocomposite Samples Obtained Using Hydrothermal Method

The preparation of nanocomposite materials with a hydrothermal method was carried out in two steps. Firstly, purified MWCNTs were dispersed in water via sonication. Then, a calculated amount of precursor of the $SnCl_2$•$2H_2O$ was dissolved in another beaker in water, whereupon 3 cm^3 HCl was added to the solution. The choice of water as a solvent, instead of e.g. ethanol, was preferably for us in the view of expected improvement in gas sensing characteristics, taking into account the fact that cover the overwhelming parts of CNTs with SnO_2 nanoparticles is ensured at that. In the next step, the MWCNT's suspension and the solution of the precursor were mixed and sonicated for 30 min. For preparing the nanocomposites, we poured the above-mentioned solutions into autoclaves, where hydrothermal synthesis was carried out at 150 ^oC for 1 day. At the end of this procedure, all obtained nanocomposite powders were filtered and dried at 90 ^oC for 5 h. The final mass ratio of the nanocomposite MWCNTs/SnO_2 obtained with the hydrothermal method in this study was 1:200, respectively. The hydrothermal synthesis process is presented in details in [12-13].

The paste for the thick film deposition made by mixing powders with α-terpineol ("Sigma Aldrich") and methanol was printed on the chemically treated surface of the alumina substrate over the ready-made Pt interdigitated electrodes. The thin-film Pt heater was formed on the back side of the substrate. Then, the obtained composite structures were cut into 3×3 mm pieces. After that, the drying and annealing processes of the resulting thick films were carried out in two stages. The first stage is the heating of thick films up to 220 ^oC with the 2 $^oC \times min^{-1}$ rate of temperature rise and holding for 3 h and then second stage: increasing in the temperature until 395 ^oC with the 1 $^oC \times min^{-1}$ rate and holding for 3 h. Further, the thick-film specimens were cooled down with the oven.

After annealing and cooling processes, the surface of MWCNTs/SnO_2 thick films was ruthenated by dipping samples into the 0.01 M $RuOHCl_3$ aqueous solution for 20 min whereupon drying at 80 ^oC for 30 min were carried out. Then, the annealing treatment was carried out again by the same method noticed above. The choice of the ruthenium as a catalyst was determined by its some advantages [12, 13, 15].

2.2. Non-Ruthenated Nanocomposite Samples Obtained by the Sol-gel Method

The powder for these samples was prepared from a 0.5 M aqueous solution of $SnCl_4 \times 5H_2O$ with the addition of MWCNTs carboxylates in a mixture of HNO_3/H_2SO_4 acids (1:3) by the sol-gel method. Thick films were obtained on the base of nanocomposite powder MWCNTs/SnO_2 with a component ratio of 1:50, respectively. All the powders were annealed at 395 ^oC for 5 hours, and then ground in an agate mortar. Multisensor platforms purchased from TESLA BLATNÁ, the Czech Republic (see Fig. 1), were used as substrates for the application of the MWCNTs/SnO_2 suspension. A thick film depositing paste was prepared using ethylene glycol as a binder. After printing on a substrate on top of the Pd-interdigitated electrodes, these samples were dried at 50 ^oC for 3 days. An annealing process was carried out with

increasing in temperature at a rate of 2 °C / min up to 234 °C and holding at this temperature for 2 hours.

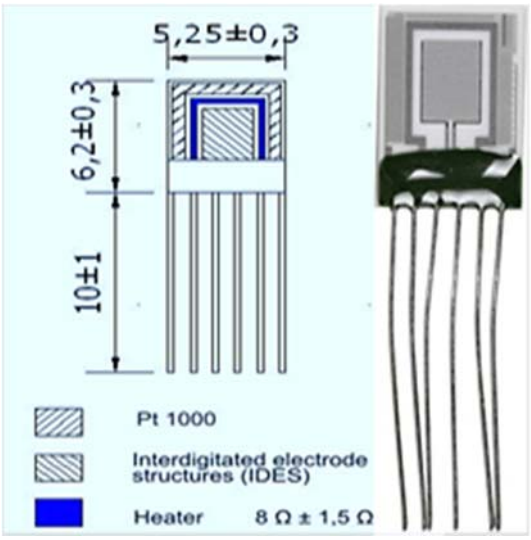

Fig. 1. The structure of the Multi-Sensor-Platform and the sensor installed on the Multi-Sensor-Platform [8].

In the final stage, the ruthenated MWCNT/SnO_2, as well as the non-ruthenated chips, were installed in the TO-5 package, and after welding the leads, the gas sensors were ready for measurements.

3. Performance of the Hydrogen Peroxide Vapors Sensors

3.1. Example About the Characteristics of the Sensors Material

The morphologies of the prepared SnO_2/MWCNT nanocomposite powders were studied by scanning electron microscopy using Hitachi S-4700 Type II FE-SEM operating in the range of 5–15 kV. The presence of an oxide layer was confirmed by SEM-EDX. Furthermore, the crystalline structure of the inorganic layer was also studied by an X-ray diffraction method using the Rigaku Miniflex II diffractometer (angle range: 2θ [°]=10–80 utilizing characteristic X-ray (CuKα) radiation). Results of these investigations were presented in [12-13] more detailed. Here, we are only noting that average crystalline size of SnO_2 nanoparticles estimated from SEM images and XRD patterns are less than 12 nm but the average diameter of non-covered by SnO_2 nanoparticles CNTs was about 40 nm.

3.2. Characteristics of Ruthenated H_2O_2 Vapor Sensors Based on MWCNTs/SnO_2

Measurement and testing of the both type developed hydrogen peroxide sensors' characteristics were carried out using program–controlled automated setup [21]. The gas response of the sensors determines as R_g/R_a, where R_g and R_a are the electrical resistance of the sensors located in the target gas/air atmosphere and pure air, respectively. The response and recovery times in each case are defined as the time required to achieve a 90 % change of the resistance, measured from the corresponding steady-state value of each signal.

The sensing characteristics were studied from 20 to 150 °C operating temperature. No appreciable gas sensitivity was observed below 70 °C and at higher than 150 °C temperatures (see Fig. 2).

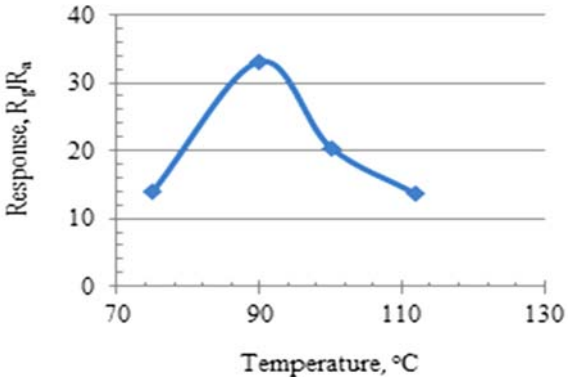

Fig. 2. Dependence of the response of the ruthenated MWCNTs/SnO_2 sensor on operating temperature.

Obviously, that the optimal operation temperature of non-ruthenated sensors is in the range of 90-100 °C. The dependence of the response of the ruthenated MWCNTs/SnO_2 (1:200) sensor on H_2O_2 vapor concentration measured at 100 °C operating temperature is shown in Fig. 3.

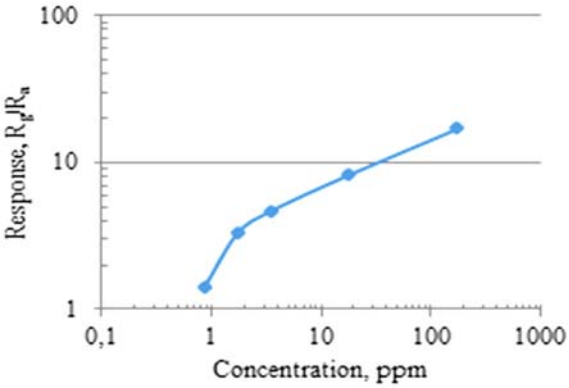

Fig. 3. Dependence of the response of the ruthenated MWCNTs/SnO_2 sensor on H_2O_2 vapor concentration.

As can be seen from Fig. 3, the linear part of the dependence of the response on the H_2O_2 vapor concentration in a double logarithmic scale extends from 2 to 120 ppm of gas concentrations. The minimal registered H_2O_2 vapor concentration is ~ 875 ppb.

3.3. Characteristics of Non-Ruthenated H_2O_2 Vapor Sensors Based on MWCNTs/SnO_2

As with the ruthenated samples, the non-ruthenated sensors show a high response in the 90-100 °C range of operating temperature. It can be seen from Fig. 4 where the sensor response vs operating temperature is presented.

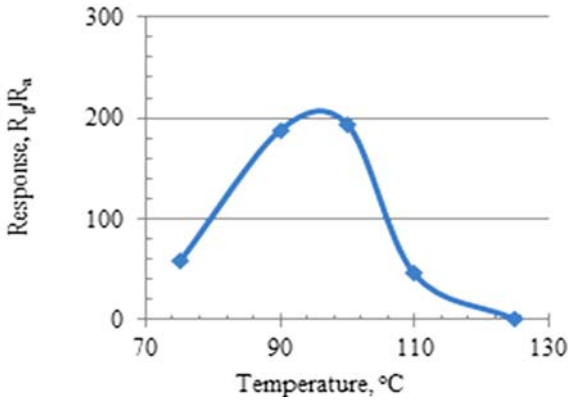

Fig. 4. Dependence of the response of the non-ruthenated MWCNTs/SnO_2 sensor on operating temperature in the presence of 12 ppm of H_2O_2 vapor in the air.

Dependence of the response of non-ruthenated MWCNTs/SnO_2 (1:50) nanocomposite H_2O_2 vapor sensor on gas concentration measured at 100 °C operating temperature is presented in Fig. 5.

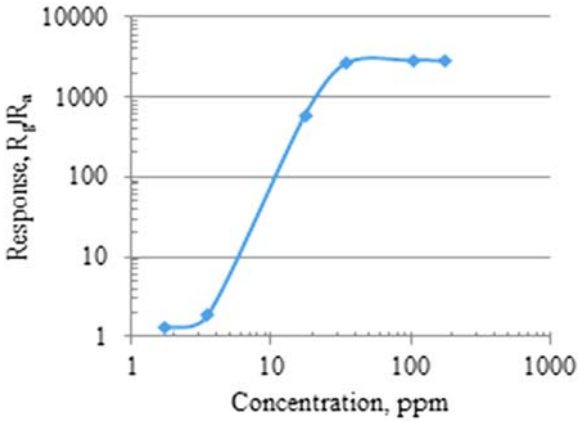

Fig. 5. Dependence of the response of non-ruthenated MWCNTs/SnO_2 sensor on H_2O_2 vapor concentration.

Obviously, a high-level signal of about three orders of magnitude and higher is characteristic for non-ruthenated samples obtained by sol-gel technology. The linear part of the response curve is in the range of gas concentrations of about 3-13 ppm. With the increase in gas concentration, the dependence of the response of non-ruthenated MWCNTs/SnO_2 sensors on H_2O_2 vapor concentration goes to saturation. The latter most likely indicates that the H_2O_2 vapor itself reaches saturation (dew point), after which the H_2O_2 vapor turns into a liquid state in the form of an aerosol in the air or starts to condense on any surface layer.

3.4. Response and Recovery Times of Studied Sensors

As an example, the response/recovery curve of the non-ruthenated H_2O_2 sensor measured at the presence of 17.5 ppm gas concentrations in the air at 100 °C operating temperature is shown in Fig 6.

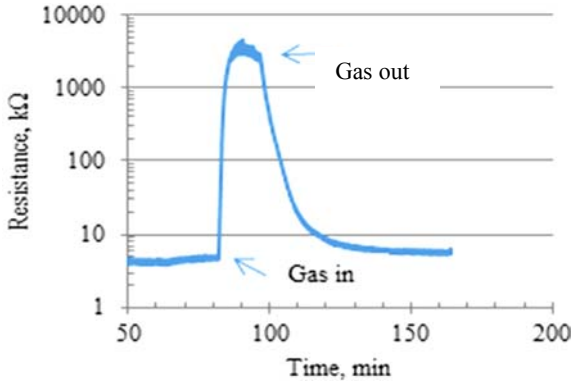

Fig. 6. The response/recovery curve of the non-ruthenated MWCNTs/SnO_2 sensor measured in the presence of 17.5 ppm H_2O_2 vapor concentrations in the air.

Dependences of response times of both types of studied sensors on H_2O_2 concentration in the air are presented in Fig. 7.

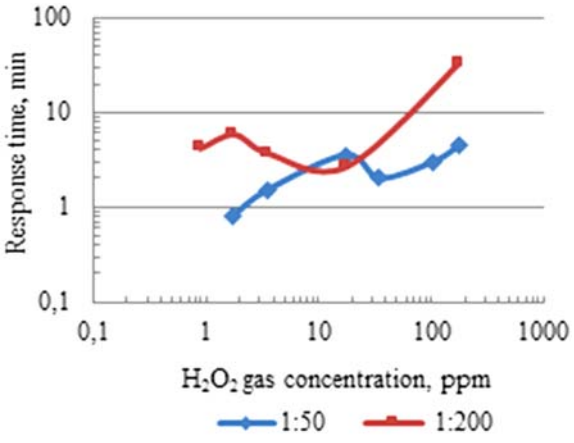

Fig. 7. Dependences of response times of both types of studied sensors on H_2O_2 concentration in the air measured at 100°C operating temperature.

Dependences of the response and recovery times of non-ruthenated and ruthenated MWCNTs/SnO_2 nanocomposite hydrogen peroxide vapor sensors on operation temperature are presented in Fig. 8 and Fig. 9, respectively. As can be seen from Fig. 8 and Fig. 9, the response time of both types of sensors varies in the range of 0.8-5 minutes. But the recovery time of non-ruthenated MWCNTs/SnO_2

sensors are significantly less than for ruthenated MWCNTs/SnO_2 sensors.

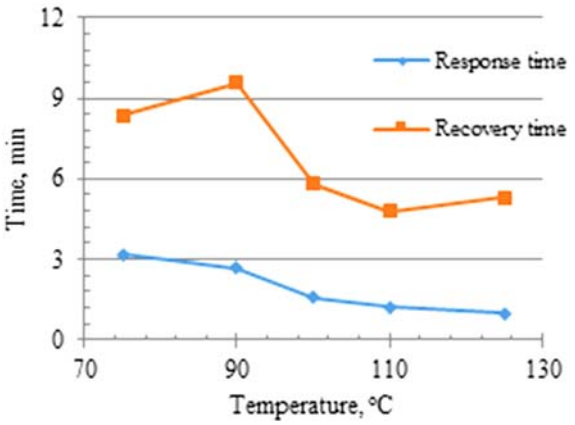

Fig. 8. Dependences of the response and recovery times of non-ruthenated hydrogen peroxide vapor sensor on operating temperature.

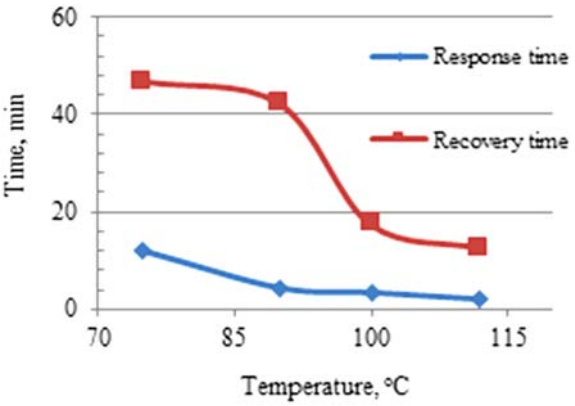

Fig. 9. Dependences of the response and recovery times of ruthenated hydrogen peroxide vapor sensor on operating temperature.

It is seen that with an increase in temperature, the response time and recovery time of both types of sensors rather sharply decrease. Given this fact, when choosing the optimal operating temperature, we preferred a temperature of 100 °C, although the response of the sensors at 90°C is slightly higher.

4. Conclusions

Thus, we developed two types of nanocomposite MWCNTs/SnO_2 hydrogen peroxide sensors, providing a response of sufficiently large amplitude in the presence of low concentrations of the target gas in the air. The minimal concentration of H_2O_2 detected by the sensors is less than 1 ppm.

The linear parts of the response dependencies on the hydrogen peroxide vapor concentration measured for ruthenated and non-ruthenated nanocomposite sensors are located in the ranges 2-120 ppm and 3-30 ppm, respectively. The response of non-ruthenated sensors is much greater than the response of ruthenated sensors. So, with an increase in the H_2O_2 vapor concentration only by one order of magnitude, the response of non-ruthenated sensors increases in three orders of magnitude, reaching 2.5×10^3 and higher. Although in terms of response and timing data, the ruthenated samples are somewhat worse in comparison with non-ruthenated ones, but they are better in terms of the threshold sensitivity, which goes into the ppb range.

Acknowledgements

This work was supported by the Swiss National Science Foundation within the framework of the SCOPES DecoComp project.

This work was presented in the 4th International Conference on Sensors Engineering and Electronics Instrumentation Advances (SEIA'2018) in Amsterdam, The Netherlands (19-21 September 2018) [22].

References

[1]. W. T. Hess, Hydrogen Peroxide in Kirk-Othmer Encyclopedia of Chemical Technology, 4th Edition, *John* Wiley & *Sons,* New York, Vol. 13, 1995.

[2]. I. Taizo, A. Sinichi, K. Kawamura, Application of a newly developed hydrogen peroxide vapor phase sensor to HPV sterilizer, *PDA Journal of Pharmaceutical Science and Technology*, Vol. 52, Issue 1, 1998, pp. 13–18.

[3]. F. Dubnikova, R. Kosloff, J. Almog, Y. Zeiri, B. R. Itzhaky, H. A. Alt, E. Keinan, Decomposition of Triacetone Triperoxide Is an Entropic Explosion, *Journal of American Chemistry Society*, Vol. 127, Issue 4, 2005, pp. 1146–1159.

[4]. S. Banerjee, S. K. Mohapatra, M. Misra, I. B. Mishra, The detection of improvised nonmilitary peroxide based explosives using a titania nanotube array sensor, *Nanotechnology,* Vol. 20, Issue 7, 2009, pp. 075502-07667.

[5]. W. Xu, Y. Fu, Y. Gao, J. Yao, T. Fan, D. Zhu, Q. He, H. Cao, J. Cheng, A simple but highly efficient multi-formyl phenol–amine system for fluorescence detection, of peroxide explosive vapour, *Chemical Communications*, Vol. 51, 2015, pp. 10868-10875.

[6]. S. Reisert, B. Schneider, H. Geissler, M. van Gompel, P. Wagner, M. J. Schöning, Multi-sensor chip for the investigation of different types of metal oxides for the detection of H_2O_2 in the ppm range, *Physica Status Solidi A*, Vol. 210, Issue 5, 2013, pp. 898–904.

[7]. S. Reisert, H. Geissler, R. Flörke, N. Näther, P. Wagner, M. J. Schöning, Towards a multi-sensor system for the evaluation of aseptic processes employing hydrogen peroxide vapour, *Physica Status Solidi A,* Vol. 208, Issue 6, 2011, pp. 1351-1356.

[8]. V. Aroutiounian, V. Arakelyan, M. Aleksanyan, G. Shahnazaryan, P. Kacer, Thin-film SnO_2 and ZnO detectors of hydrogen peroxide vapors, *Journal of*

Sensors and Sensors Systems, Vol. 7, Issue 1, 2018, pp. 281–288.

[9]. D.-J. Lee, S.-W. Choi, Y. T. Byun, Room temperature monitoring of hydrogen peroxide vapor using platinum nanoparticles-decorated single-walled carbon nanotube networks, *Sensors and Actuators B: Chemical,* Vol. 256, 2018, pp. 744–750.

[10]. A. L. Verma, S. Saxena, G. S. S. Saini, V. Gaur, V. K. Jain, Hydrogen peroxide vapor sensor using metal-phthalocyanine functionalized carbon nanotubes, *Thin Solid Films*, Vol. 519, Issue 22, 2011, pp. 8144–8148.

[11]. F. I. Bohrer, C. N. Colesniuc, J. Park, I. K. Schuller, A. C. Kummel, W. C. Trogler, Selective Detection of Vapor Phase Hydrogen Peroxide with Phthalocyanine Chemiresistors, *Journal of American Chemical Society*, Vol. 130, Issue 12, 2008, pp. 3712-3713.

[12]. V. M. Aroutiounian, A. Z. Adamyan, E. A. Khachaturyan, Z. N. Adamyan, K. Hernadi, Z. Pallai, Z. Nemeth, L. Forro, A. Magrez, E. Horvath, Study of the surface-ruthenated SnO_2/MWCNTs nanocomposite thick-film gas sensors, *Sensors and Actuators B: Chemical*, Vol. 177, 2013, pp. 308–315.

[13]. V. Aroutiounian, Z. Adamyan, A. Sayunts, E. Khachaturyan, A. Adamyan, K. Hernadi, Z. Nemeth, P. Berki, Comparative Study of VOC Sensors Based on Ruthenated MWCNT/SnO_2 Nanocomposites, *International Journal of Emerging Trends in Science and Technology*, Vol. 1, Issue 8, 2014, pp. 1309-1319.

[14]. Z. Adamyan, A. Sayunts, V. Aroutiounian, E. Khachaturyan, A. Adamyan, M. Vrnata, P. Fitl, J. Vlček, Study of Propylene Glycol, Dimethylformamide and Formaldehyde Vapors Sensors Based on MWCNTs/SnO_2 Nanocomposites, *Sensors & Transducers*, Vol. 213, Issue 6, 2017, pp. 38-45.

[15]. Z. N. Adamyan, A. G. Sayunts, E. A. Khachaturyan, V. M. Aroutiounian, Study of nanocomposite thick-film butanol vapor sensors, *Journal of Contemporary Physics (Armenian Academy of Sciences*), Vol. 51, Issue 2, 2016, pp. 143-149.

[16]. N. Sinha, J. Ma, J. T. W. Yeow, Carbon Nanotube-Based Sensors, *Journal of Nanoscience and Nanotechnology*, Vol. 6, Issue 3, 2006, pp. 573-590.

[17]. R. Leghrib, A. Felten, J. J. Pireaux, E. Llobet, Gas sensors based on doped- CNT/SnO_2 composites for NO_2 detection at room temperature, *Thin Solid Films*, Vol. 520, Issue 3, 2011, pp. 966–970.

[18]. M. Penza, R. Rossi, M. Alvisi, G. Cassano, M. A. Signore, E. Serra, R. Giorgi, Pt and Pd-nanoclusters functionalized carbon nanotubes networked films for sub ppm gas sensors, *Sensors and Actuators B: Chemical*, Vol. 135, Issue 1, 2008, pp. 289–297.

[19]. M. Penza, G. Cassano, R. Rossi, M. Alvisi, A. Rizzo, M. A. Signore, T. Dikonimos, E. Serra, R. Giorgi, Enhancement of sensitivity in gas chemiresistors based on carbon nanotube surface functionalized with noble metal (Au, Pt) nanoclusters, *Applied Physics Letters*, Vol. 90, 2007, pp. 173123-1–173123-3.

[20]. M. S. Wagh, G. H. Jain, D. R. Patil, S. A. Patil, L. A. Patil, Surface customization of SnO_2 thick films using RuO_2 as a surfactant for the LPG response, *Sensors and Actuators B: Chemical*, Vol. 122, Issue 2, 2007, pp. 357–364.

[21]. Z. Adamyan, A. Sayunts, V. Aroutiounian, E. Khachaturyan, M. Vrnata, P. Fitl, J. Vlček, Nanocomposite sensors of propylene glycol, dimethylformamide and formaldehyde vapors, *Journal of Sensors and Sensors Systems*, Vol. 7, Issue 1, 2018, pp. 31–41.

[22]. Z. N. Adamyan, A. G. Sayunts, E. A. Khachaturyan, V. M. Araqelyan, V. M. Aroutiounian, B. Joost, Study of MWCNTs/SnO_2 Nanocomposite H_2O_2 Vapor Sensors, in *Proceedings of the 4th International Conference on Sensors Engineering and Electronics Instrumentation Advances (SEIA'18)*, Amsterdam, Netherlands, 19-21 September 2018, pp. 53-56.
